Journal of Composite Materials

http://jcm.sagepub.com

An Improved Cohesive Zone Model for Residual Notched Strength Prediction of Composite Laminates with Different Orthotropic Lay-Ups

C. S. Shin and C. M. Wang

Journal of Composite Materials 2004; 38; 713
DOI: 10.1177/0021998304031635

The online version of this article can be found at:
http://jcm.sagepub.com/cgi/content/abstract/38/9/713

Published by:
SAGE
http://www.sagepublications.com

On behalf of:
American Society for Composites

An Improved Cohesive Zone Model for Residual Notched Strength Prediction of Composite Laminates with Different Orthotropic Lay-ups

C. S. SHIN* AND C. M. WANG
Department of Mechanical Engineering
National Taiwan University
No. 1, Sec. 4, Roosevelt Rd., Taipei, Taiwan

ABSTRACT: The traditional methods employing a characteristic length approach to predict residual strength of notched laminates did not recognize damage development prior to final failure. Due to this lack of physical basis, re-calibration is often needed when the specimen geometry and size are changed. More recent models such as the Damage Zone Model (DZM), Cohesive Zone Model (CZM) and the Effective Crack Growth Model (ECGM), have recognized the occurrence of progressive material softening ahead of the notch tip prior to catastrophic failure. However, since the anisotropic characteristic of the composite laminate has not been properly accounted for, these models may not be widely applicable for the laminates with different degrees of anisotropy. In this study, an Improved Cohesive Zone Model (ICZM) with proper consideration for anisotropy is proposed to predict the notched strength of composite laminate. Based on three fundamental parameters: namely the unnotched strength σ_0, the apparent fracture energy G_c and the effective longitudinal stiffness E', this model successfully predicted the strength of notched composite laminates with various degrees of anisotropy. The current model also gives accurate prediction of the progressive damage zone size in quasi-isotropic and cross-ply laminates.

KEY WORDS: fictitious crack growth, residual strength, notched composite laminates, cohesive stress, anisotropic characteristic.

INTRODUCTION

NOTCHED STRENGTH PREDICTION in composite materials has been widely studied since the 1970s [e.g., 1–7]. Early approaches are often empirical in nature and have virtually no reference to the physical damage mechanisms. Whitney and Nuismer [1,2] proposed the

*Author to whom correspondence should be addressed. E-mail: csshin@ccms.ntu.edu.tw

0021-9983/04/09 0713–24 $10.00/0 DOI: 10.1177/0021998304031635

point stress criterion (PSC) and the average stress criterion (ASC). The PSC assumes failure to occur when the stress at a characteristic distance ahead of the notch tip reaches the unnotched strength, σ_0. The point stress is replaced by the average stress over the characteristic distance in the ASC. While these models are simple to apply and give reasonable accuracy, their physical basis is not sound. For example, they employed the elastic stress distribution of the virgin specimen for calculation. Damage inevitably occurs prior to fracture and will cause stress redistribution ahead of the notch. Moreover, such redistribution will depend on the specimen geometry and stacking sequence. Re-calibration of the characteristic distance is therefore often needed if any parameter such as notch acuity or notch depth to specimen width ratio is changed. Alternatively, more degrees of freedom were introduced to improve agreement with experimental data by including additional curve fitting parameters [3–6]. This technique has in fact been employed by a number of workers such as Karlak [3], Pipes et al. [4], and Tan [5,6]. Mar and Lin [7] proposed an alternative model based on the concept of fracture mechanics. It employs two artificial parameters: composite fracture toughness and singularity. Both parameters were determined by the best fit to the whole set of experimental data. Early work on notched strength prediction is comprehensively reviewed by Awerbuch and Madhukar [8].

Since the 1980s, more attention was paid to the physical damage mechanism that progressively softens material ahead of the notch tip prior to catastrophic failure. Bäcklund et al. [9,10] proposed the damage zone model (DZM) in which the damage zone ahead of notch tip was viewed as a line-crack with cohesive stress acting on the crack surfaces to simulate the weakened material. Its evaluation was based on finite element analysis, and only the unnotched strength, stiffness and an apparent fracture energy are required as input. Although good accuracy had been achieved, it may well be due to the fact that the value of the apparent fracture energy was so chosen as to ensure agreement with the experimental data. In order to simplify the analysis procedures, Eriksson and Aronsson [11] proposed an alternate damage zone criterion (DZC), which was based on force equilibrium and the Dugdale strip yield model [12] in the damage zone. However, such model needs a set of experimental data to calibrate the damage zone and therefore fell in line with the characteristic length approach. Based on the DZM, Afaghi-Khatibi et al. [13–15] proposed the effective crack growth model (ECGM). By means of equilibrium between the applied load and the resultant axial force acting on the net-section plane of the laminate, the damage growth with the applied load and stress distribution can be obtained using an iterative technique. However, there are some points which call for clarification on detailed examination of their algorithm. Firstly, in [13] the net-section stress distribution has a big discontinuous decrease when crossing from the damaged zone into intact region. No such discontinuity was employed in [14,15] even though the geometrical and loading configurations were the same. Secondly, the crack opening displacement (COD) expression employed was that for small edge cracks in a relatively large plate. However, most of the critical damage zones or ''fictitious crack'' sizes were close to or larger than the hole diameter. If a consistent stress distribution and more accurate COD formulation have been employed, it is not clear whether the current good accuracy can still hold or not.

By using the progressive damage methodology, Chang et al. [16–18] proposed the progressive damage model. In this model, finite element method is adopted to perform stress analysis. The results were used to decide whether damage has occurred or not. If damage occurs, the elastic constants of the damaged element will be

degraded according to its damage mode. Such progressive degradation of elastic constants can simulate the damage process in composites very well and predict the notched residual strength fairly accurately. However, because the evaluation of the progressive damage methodology is based on the expensive and time-consuming finite element analysis, it is less attractive than other closed form criteria such as the one described in this work.

Based on the stress redistribution phenomenon as pointed out in the DZM, Soutis et al. [19] proposed the cohesive zone model (CZM) for compression fracture of notched T800/924C $[\pm 45/0_2]_{3S}$ composite laminate. In this model, the correlation between applied stress and damage zone can be expressed in a closed form and the residual strengths were predicted with good accuracy. Furthermore, the predicted damage zone size agreed with the observed microbuckling zone. However, in their formulation, isotropic expressions for the stress intensity and COD had been used for the obviously anisotropic material. Application had been demonstrated on the compressive failure of one particular stacking sequence. Whether this isotropic formulation will be successful for laminate with different lay-up configurations and for tensile loading is worth further studying. Following the line of argument as the CZM, in this study an improved cohesive zone model (ICZM) taking into account of anisotropy was developed to evaluate the tension fracture of laminate with different lay-up. It was found that notched strength could be simulated with good accuracy for composite laminates with arbitrary lay-ups.

IMPROVEMENT ON THE COHESIVE ZONE MODEL (ICZM)

Linear Softening Cohesive Zone Model (CZM) of Soutis et al. [14]

Soutis et al. [19] have developed the CZM for the initiation and growth of compressive damage from the edge of a blunt notch such as a hole. This model treated the materials as macroscopically homogenous and isotropic. It assumed that microbuckling initiates when the concentrated compressive stress at the hole edge equals the unnotched strength σ_0. Damaged region was viewed as a line-crack, not free to "close" as there was reactive "cohesive" stress acting on it, as shown in Figure 1. Microbuckling zone spreading forward with increasing compressive load was modeled by the growth of the apparent crack. The evolution of microbuckling or crack growth was determined by invoking the fact that the stress should remain finite everywhere [20]. This required the total stress intensity factor (SIF), K_{total}, which was comprised of the stress intensity factors due to the remote stress (K_S) and that due to the cohesive stress (K_σ), as illustrated in Figure 2. They assumed the crack interfaces form a negative "crack opening displacement" under the remote compressive stress S. This gave rise to reactive cohesive stress tending to open the crack. The cohesive stress was related to the COD through the linear traction displacement relationship [21] (see Figure 1(a) and (b)). During calculation the crack was discretised into a number of n segments. The cohesive stress σ was assumed to be uniformly distributed within each segment. As the crack advances, the number of segments increases. For an assumed length of equivalent crack l, the remote stress S was obtained by iteration so that the finite stress criterion was satisfied. The algorithm was detailed in [19]. The remote stress S can be expressed as a function of crack length l, unnotched strength σ_0, critical crack opening

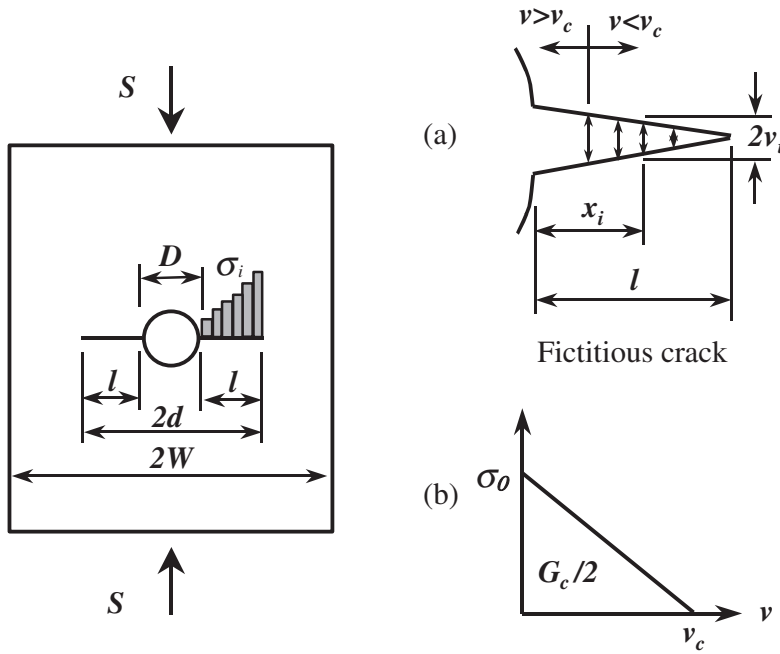

Figure 1. *Damage zone is viewed as a line-crack with cohesive stress acting on its surfaces: (a) fictitious crack with cohesive stress and (b) linear relationship between cohesive stress and crack opening displacement.*

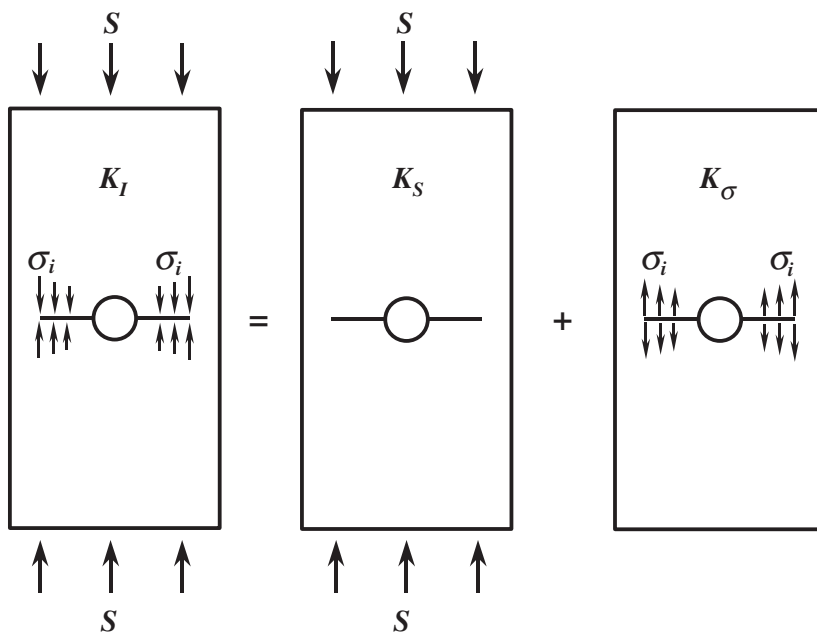

Figure 2. *Superposition for a notched plate with cohesive stress acting on the two radial crack surfaces.*

displacement (COD) v_c, elastic stiffness E, and geometry (plate width W and hole diameter D), i.e.

$$S = \sum_{i=1}^{n} \beta_i \sigma_i = f(l, \sigma_0, v_c, E, D, W) \tag{1}$$

where β_i and σ_i were also given in [19]. This model required the knowledge of two empirical parameters: the unnotched strength (σ_0) and the critical COD (v_c). The latter is related to the measured fracture energy G_c through the assumed linear traction–crack displacement curve (see Figure 1(b)).

Improved Cohesive Zone Model (ICZM)

For an anisotropic body, Konish [22] pointed out that the influence of material anisotropy on the SIF is dependent on both the specimen geometry and laminate configuration, as well as the material properties. For the center-cracked laminate with $[\pm 45]_{4S}$ lay-up where anisotropy has the largest influence, the anisotropic SIF is within 6% of its isotropic counterpart when the crack length to specimen width aspect ratio is equal to 0.5. It therefore seems reasonable to use the isotropic SIF in place of its anisotropic counterpart to a first approximation. However, the COD is sensitive to anisotropy. To correctly describe it, the Young's modulus E for an isotropic body has to be replaced by the effective longitudinal stiffness E' in the COD expression (see Appendix).

$$E' = \frac{1}{\sqrt{1/(2E_{11}E_{22})\left[(E_{11}/E_{22})^{1/2} - \nu_{12} + (E_{11})/(2G_{12})\right]}} \tag{2}$$

where E and G are the laminate in-plane extensional and shear moduli respectively, and ν is the Poisson's ratio (1 = loading axis, 2 = transverse axis).

From the above discussion, it is apparent that the CZM would incur considerable error if it was applied to an anisotropic composite laminate with an arbitrary stacking sequence. In the current improved model (ICZM), the materials are also viewed as macroscopically homogenous but the effect of anisotropy on the COD will be taken into account. Moreover, the applied loading is tensile which makes the phenomenon of crack opening and cohesive restraint logically more sensible.

By replacing E with E' in Equation (1), the remote stress S can be expressed as

$$S = \sum_{i=1}^{n} \beta_i \sigma_i = f(l, \sigma_0, v_c, E', R, W) \tag{3}$$

Using Equation (3), the residual strength of a notched composite laminate with varying degrees of orthotropy can be predicted. In this model, only three parameters, σ_0, v_c and E' are needed. σ_0 can be measured from unnotched coupons, v_c can be determined by measuring the fracture energy G_c of the laminate and E' calculated from the relevant elastic constants. In other words, all the required material parameters are measured,

leaving no room for arbitrary parameter adjustment or curve fitting to ensure agreement between the numerical predictions and observed residual strengths.

MATERIALS AND EXPERIMENTAL DETAILS

A thermoplastic AS4/PEEK (material 1) and a thermosetting T300/3501 (material 2) were used in the current study. For each material, the unidirectional prepregs were laid up in quasi-isotropic $[0/45/90/-45]_{2S}$ (laminates Q1 and Q2), cross-ply $[0/90]_{4S}$ (laminates C1 and C2) and angle-ply $[\pm 45]_{4S}$ (laminates A1 and A2). Fabrication employed a diaphragm type forming mold and was done according to the curing cycles recommended by the respective manufacturers. The resulting nominal thicknesses of AS4/PEEK and T300/3501 are 2.1 and 2.4 mm, respectively. All specimens were cut using water mist-cooled diamond-coated wheels. The dimensions of both the unnotched and notched specimens are 210 mm long and 25.4 mm wide. To alleviate damage induced during drilling, specimens were sandwiched between two sacrificial plates. Water-cooled Ti-coated high-speed steel drills were used for hole machining. Four hole diameters (D), 3, 6.3, 9.5, and 12.0 mm, to give diameter to specimen width (W) ratios (D/W) of 0.12, 0.25, 0.37, and 0.47 were employed. Integrity of the specimens was checked before testing by Ultrasonic C-scan with a 15 MHz probe. Woven glass/epoxy end-tab of length 45 mm were glued to both ends of the specimen using cyanoacrylic adhesive for gripping.

The elastic constants of the unidirectional composites of both materials are listed in Table 1. In addition to our own results, data collected from the literatures have also been adopted to examine the current model. The elastic constants of the unidirectional composites of these laminates are also listed in Table 1. For laminates Q3 and Q4, the unidirectional prepregs of T300/1034 [10] and T300/914C [11] were laid up in $[0/90/\pm 45]_{2S}$ and $[(\pm 45/0/90)_3/0/90/\pm 45]_S$, respectively. For laminates C3 and C4, Scotchply 1002 [2] and T300/5208 [2] were both laid up in $[0/90]_{4S}$. All tests on our own laminates (Q1, Q2, C1, C2, A1, and A2) were performed on an MTS 810 servo-hydraulic machine at room temperature with a constant displacement rate of 2 mm/min. The mean unnotched strengths and fracture energies for these materials with various lay-ups are listed in Table 2. The unnotched strength is the average of ten data whereas the notched strength is the average of at least three data. The fracture energy is the average of three data and was measured from the standard central slit coupon specimen with different slit length to width ratios [23,24]. For the laminates (Q3, Q4, C3, and C4) collected from the literatures, their fracture energies were also calculated likewise.

Table 1. Elastic constants of various composite laminae examined.

Materials	Laminates	E_{11} (GPa)	E_{22} (GPa)	G_{12} (GPa)	ν_{12}
AS4/PEEK	Q1, C1, A1	141.0	10.0	5.1	0.30
T300/3501	Q2, C2, A2	144.5	8.7	5.7	0.28
T300/1034 [8]	Q3	138.0	11.0	4.0	0.35
T300/914C [9]	Q4	138.0	9.0	3.1	0.35
Scotchply 1002 [2]	C3	38.5	8.3	4.1	0.26
T300/5208 [2]	C4	147.6	11.0	5.3	0.29

Table 2. The mechanical properties of various composite laminates examined.

Materials	Laminates	Lay-up	σ_0 (MPa)	G_c[a] (kJ/m^2)	E_{11}[b] (GPa)	E'_{11}[c] (GPa)
AS4/PEEK	Q1	$[0/45/90/-45]_{2S}$	800	56	54.5	54.5
	C1	$[0/90]_{4S}$	1228	77	75.9	37.0
	A1	$[\pm 45]_{4S}$	394	42	18.1	37.0
T300/3501	Q2	$[0/45/90/-45]_{2S}$	685	40	55.7	55.7
	C2	$[0/90]_{4S}$	992	66	76.9	39.0
	A2	$[\pm 45]_{4S}$	254	12	19.8	39.0
T300/1034	Q3	$[0/90/\pm 45]_{2S}$	581	45	52.9	52.9
T300/914C	Q4	$[(\pm 45/0/90)_3/0/90/\pm 45]_S$	548	36	51.4	51.4
Scotchply 1002	C3	$[0/90]_{4S}$	423	41	23.6	17.2
T300/5208	C4	$[0/90]_{4S}$	637	80	80.0	38.7

[a] G_c is determined by measuring the fracture toughness of the specimen with a central crack, except laminate Q3 where single edge cracked specimens were used [19].
[b] E_{11} is calculated from the basic mechanical properties of the composite lamina, as listed in Table 1.
[c] E'_{11} is calculated by using Equation (2), in which E_{11}, E_{22}, G_{12}, and ν_{12} are also calculated from the basic mechanical properties of the composite laminae, as listed in Table 1.

EVALUATION OF THE NEW MODEL

In this section, the residual strengths of laminates are compared against the predictions using the ICZM as well as the predictions from other semi-empirical models including PSC, ASC, and DZC. All laminates were tested at room temperature except Q4, which was tested at 100°C. The required mechanical properties of all these laminates have been listed in Table 2. It is hoped that the effectiveness of the current model can be more thoroughly evaluated with this wide range of configurations.

Notched Strength Predictions by the Existing Models

A characteristic length has been employed in a number of existing models. These are characteristic lengths d_0 for PSC, a_0 for ASC, and a critical damage length d_I^* for DZC. Whitney and Nuismer [1,2] proposed that the characteristic length is independent of notch acuity. In the current study, these parameters were determined from the specimens with a central slit, except for the laminate Q4 whose characteristic lengths were determined from single-edge cracked specimens [23,24]. The set of characteristic parameters for each laminate system are listed in Table 3.

The residual strengths of the above laminates predicted using the existing models are compared against experimental data, as shown in Figures 3–7. For our own laminates (Q1, Q2, C1, C2, A1, and A2), the widths of specimen were fixed (25.4 mm) and the hole diameters were varied from 3 to 12 mm. In Figure 3(a)–(f), the horizontal and vertical axes represent the hole diameter (D) and the normalized notched residual strength (σ_N/σ_0), respectively. These axes were so chosen as to reveal any correlation between D and σ_N/σ_0. Regarding the data collected from the literatures: two sets of specimens were tested for laminate Q3. For each set the diameter D was fixed and the width W was varied (see Figure 4). Hence the width W is employed for the horizontal axis. For laminates Q4, both D and W were altered to obtain the same D/W (=0.167). For laminates C3 and C4, two

sets of D/W (= 0.1 and 0.3) were obtained by varying both D and W. For these laminates, D is used for the horizontal axis and the width W of each set of data is indicated in the figures (see Figures 5–7).

As previously reported [25,26], the residual strengths of each laminate decreased with increasing hole diameters. For the laminates with quasi-isotropic lay-up (Q1-Q4), PSC, ASC, and DZC give maximum errors of 15, 10, and 20%, respectively (see Figure 3(a) and (b), 4, and 5). It is worth pointing out that the DZC tends to give larger errors with increasing hole diameters. For the laminates with cross-ply lay-up (C1-C4), PSC, ASC and DZC give maximum errors of 33, 14, and 32%, respectively (see Figures 3(c) and (d), 6, and 7). For laminate C4, Nuismer and Whitney [2] deemed the residual strength of the

Table 3. Characteristic parameters of different composite laminates for residual strength prediction using PSC, ASC, and DZC [19].

		Characteristic Parameters		
Materials	**Laminates**	**PSC d_0 (mm)**	**ASC a_0 (mm)**	**DZC d_l^* (mm)**
AS4/PEEK	Q1	0.60	2.90	0.70
	C1	0.23	0.99	0.24
	A1	1.50	7.45	3.00
T300/3501	Q2	0.44	1.99	0.48
	C2	0.38	1.71	0.41
	A2	1.29	6.20	2.14
T300/1034	Q3	0.97	2.27	1.30
T300/914C	Q4	0.98	4.55	1.17
Scotchply 1002	C3	0.42	1.94	0.46
T300/5208	C4	0.70	3.52	0.85

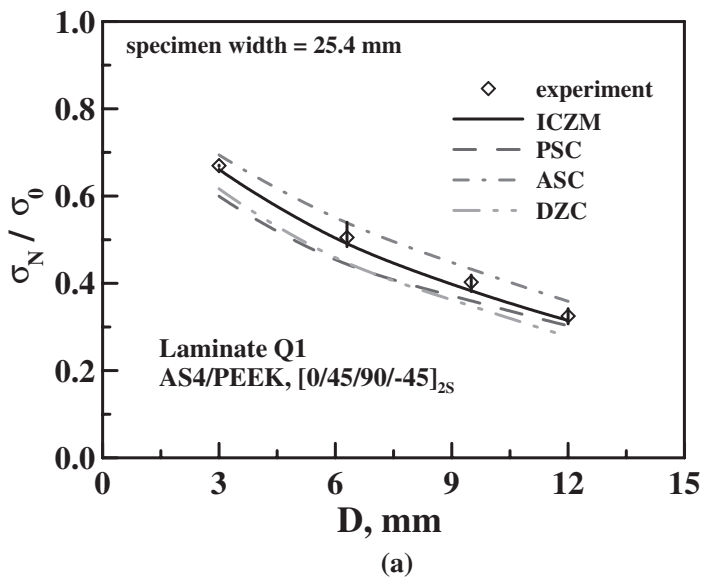

Figure 3. *Residual strength predictions of quasi-isotropic laminates: (a) laminate Q1, (b) laminate Q2, (c) laminate C1, (d) laminate C2, (e) laminate A1, and (f) laminate A2.*

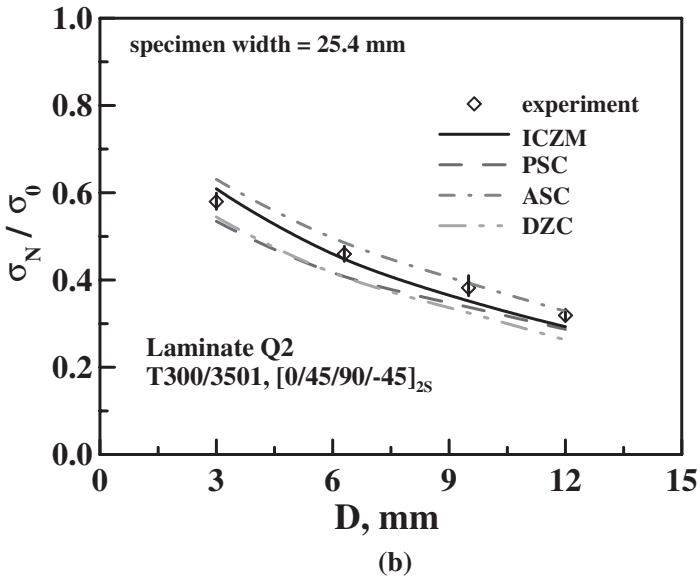

(b)

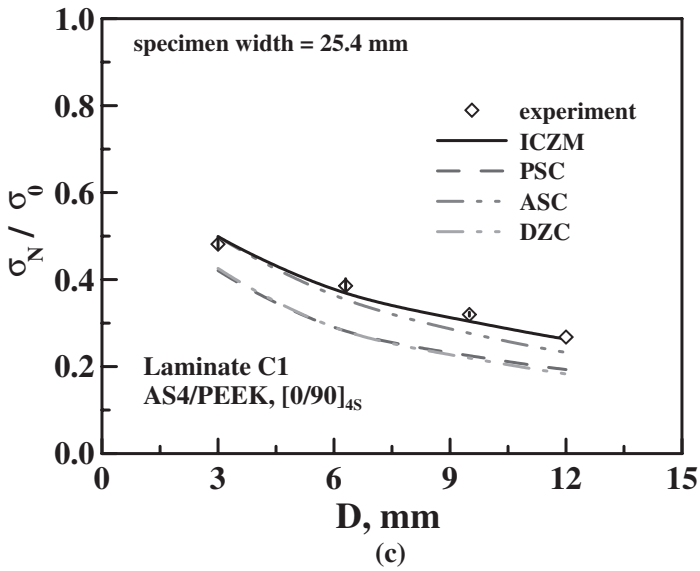

(c)

Figure 3. *Continued.*

76-mm wide specimen with 25.4 mm hole problematic and so this result will be excluded from later comparisons. For the laminates with angle-ply lay-up, PSC, ASC, and DZC give maximum errors of 13, 26, and 17%, respectively (see Figure 3(e) and (f)).

The characteristic parameters of each semi-empirical model are assumed to be material constants [1,2,8]. However, the above predictions reveal that the characteristic parameters obtained from the specimen with a central slit [23,24] cannot guarantee the accuracy of residual strength prediction in the specimens with a circular hole. In fact, re-calibration of the characteristic parameter is often needed if any parameter such as notch acuity or notch

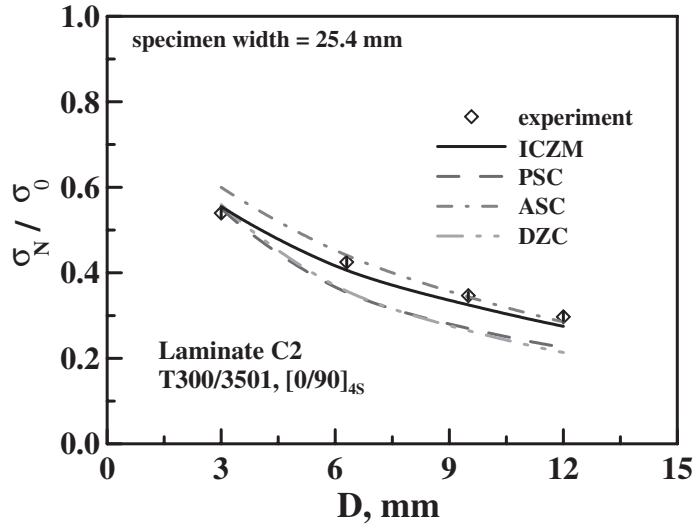

(d)

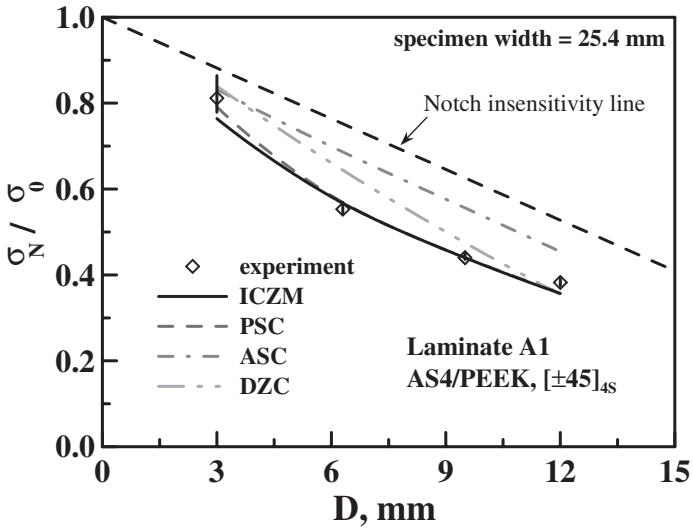

(e)

Figure 3. *Continued.*

depth to specimen width ratio is changed [27]. In order to obtain more prediction, averaged characteristic length from a large amount of specimens with different geometric configurations is sometimes adopted [8]. However, if the parameter does not correctly represent the "characteristic" of the physical damage, accuracy cannot be guaranteed even if the averaged parameter is used. For example, Coats and Harris [28] studied the AS4/3501-6 $[\pm 45/0/90/\pm 30/0]_S$ laminate with four different slit lengths and widths. The widths and slit lengths in centimeter are: 10.16×1.27, 10.16×2.54, 30.5×7.62, and 91×22.86. If we use the results from the first two batches of specimens to generate an

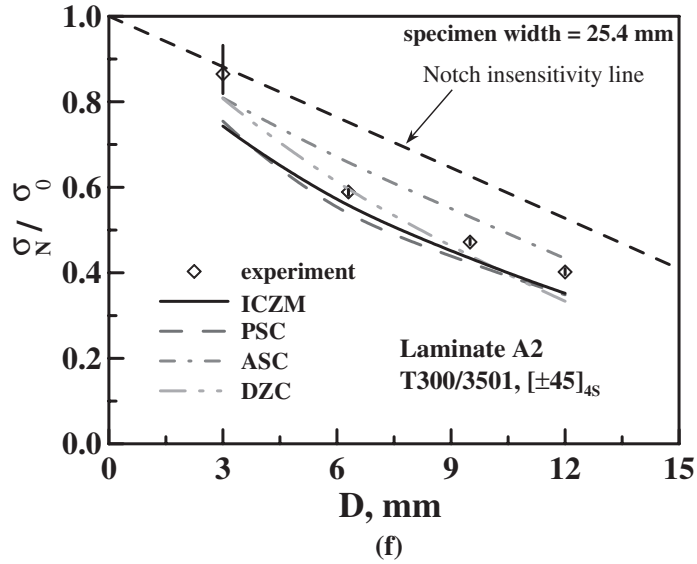

Figure 3. *Continued.*

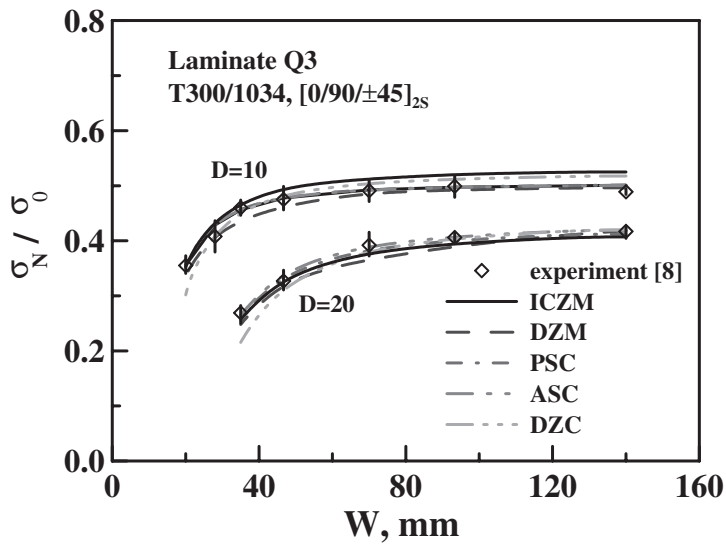

Figure 4. *Residual strength predictions of laminate Q3 [8].*

average characteristic length and use the PSC to predict the residual strength of the laminate with 91 cm width, an 80% overestimation occurred. This suggests using small laboratory scale specimens to evaluate integrity of large structures via empirical models such as PSC can be dangerously un-conservative. Such error is expected as different remaining ligament lengths lead to different degrees of elastic stress redistribution ahead of notch tip. If the laminate configuration of laboratory specimens is different from that of a practical structure, such error may be aggravated. Therefore, it is necessary to develop a

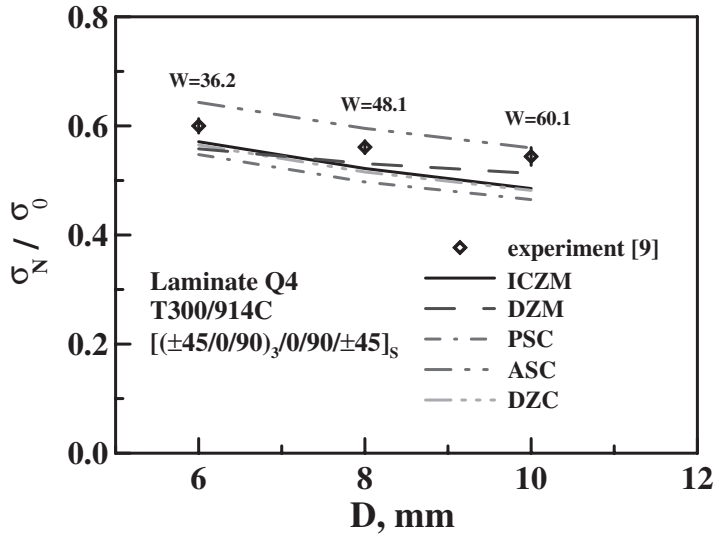

Figure 5. *Residual strength predictions of laminate Q4 [9].*

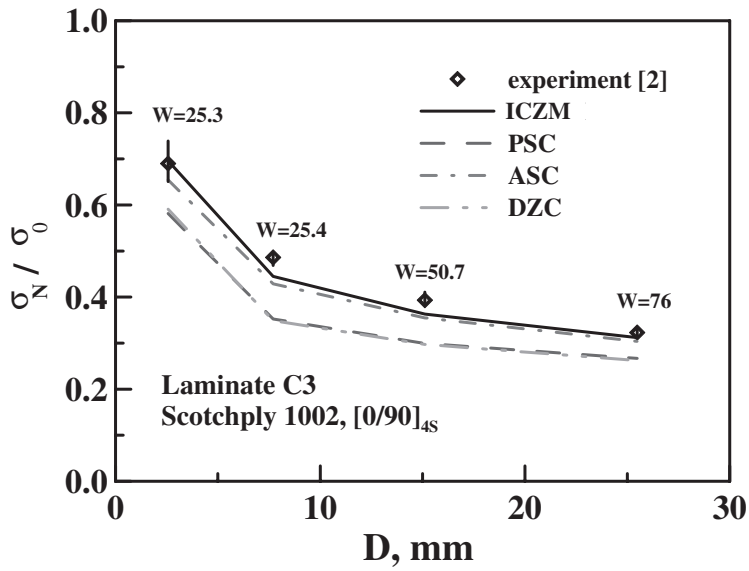

Figure 6. *Residual strength predictions of laminate C3 [2].*

new model that reasonably represents the "characteristic" of the physical damage. If such representation can be achieved, this new model will be able to give accurate prediction for different laminate geometrical configurations and stacking sequences.

For laminates Q3 and Q4, the predictions by the DZM are available and have therefore been included for comparison (see Figures 4 and 5). It is obvious that no semi-empirical model is generally applicable to all laminates. The DZM gives better predictions than the semi-empirical models, at the expense of tedious finite element analysis.

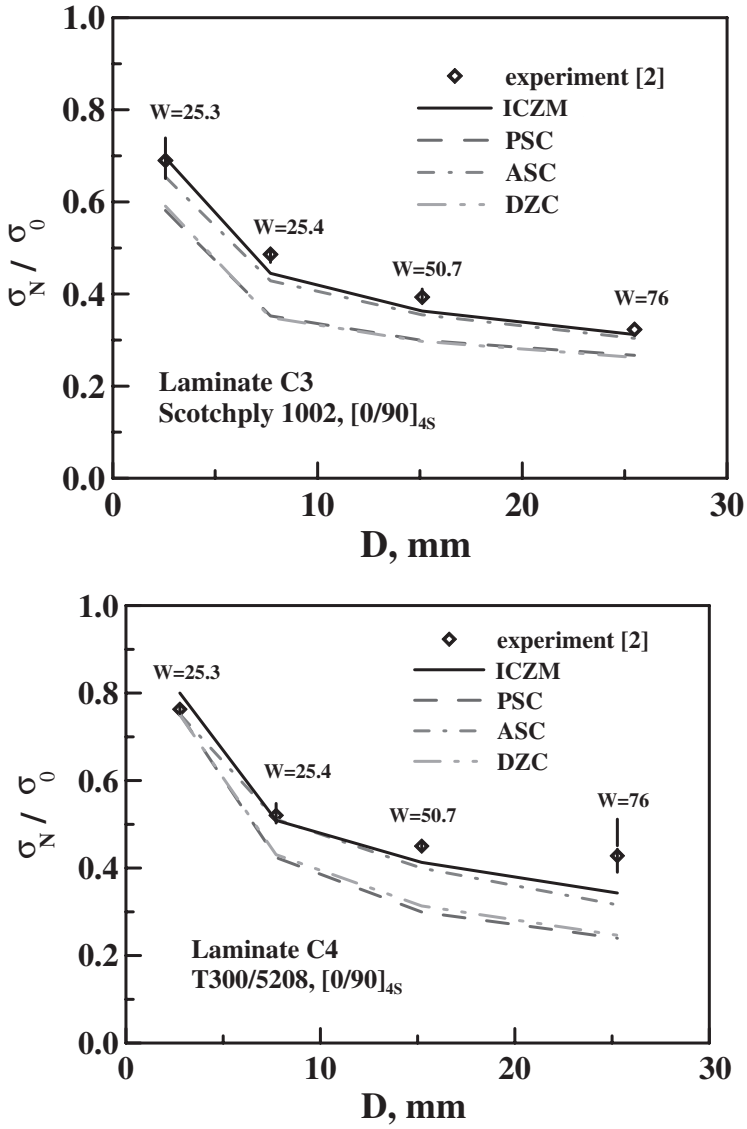

Figure 7. *Residual strength predictions of laminate C4 [2].*

Notched Strength Predictions by the ICZM

To assess the residual strength of notched composite laminate using this new model, the only material parameters needed are the effective longitudinal stiffness E', the unnotched tensile strength σ_0, and the fracture energy G_c. E' were calculated from the elastic properties of laminae (see Table 1) using Equation (2). σ_0 were measured using standard strength test method [29], and G_c were determined from the standard fracture test using the coupon specimens with a central slit [2,10,23,24].

Predictions from the ICZM are also compared with the experimental data in Figures 3–7. For our own quasi-isotropic and cross-ply laminates (Q1, Q2, C1, and C2),

the largest error incurred by the FCGM is −8.1% (see Figure 3(a)–(d)). This is comparable to those incurred by the semi-empirical models. The residual strengths of angle-ply laminates A1 and A2 tend to be notch insensitive. Notch insensitivity is represented by the dashed-line ($\sigma_N/\sigma_0 = 1 - D/W$) in Figure 3(e) and (f). This phenomenon may be attributed to the strongly nonlinear stress–strain response of the angle-ply lay-up. Even then the ICZM gives a maximum error of −6.7 and −14.1%, respectively for laminates A1 and A2. These are more favorable than the 26 and −27% incurred by the previous semi-empirical models. The above comparison suggests that the ICZM gives accurate predictions and is applicable to widely different lay-ups.

For laminate Q3, residual strengths for laminates with two different hole diameters (10 and 20 mm) and a wide range of widths were reported [10]. Laminate Q4 were tested at 100°C for a series of width and hole diameter combinations [11]. The ICZM gives a maximum error of 7.4 and 10.8% for laminates Q3 and Q4, respectively. These compared well with the 7.8 and 7.0% given by the more tedious DZM (see Figures 4 and 5). Favorable predictions on Q3 and Q4 suggest that the ICZM is not only adequate for a wide range of specimen widths but also for high temperature applications. For laminates C3 and C4, both the widths and hole diameters of the specimens are also varied [2]. Excluding the previously mentioned questionable experimental data of laminate C4, the FCGM gives a maximum error of −8.5 and −8.3% for laminates C3 and C4, respectively (see Figures 6 and 7). Such results are much more accurate than that provided by the PSC, ASC, and DZC. Besides, it is worthwhile to mention that the ICZM can also be used to predict the residual strength of the laminate with a sharp slit [23,24]. For the AS4/3501-6 $[\pm 45/0/90/\pm 30/0]_S$ laminate [28] with a central slit, the ICZM only gives 9% error on the laminate with 91 cm width and the maximum error for all four geometries is around 14% [23,24]. These compare favorably with the previously quoted 80% error if prediction was made using the PSC.

Table 4 summarizes the maximum prediction errors by each model on all the laminates tested. It is clear that the current ICZM stands out to have the best all-round accuracy.

Table 4. Comparison of the maximum percentage errors between measured notched strengths and those predicted using different models.

Materials	Laminates	Anisotropy Factor *H*	Maximum % Error between Prediction and Measured Notched Strengths[a]					
			PSC	ASC	DZC	DZM[b]	ICZM	CZM
AS4/PEEK	Q1	1.00	−12.2	10.4	−14.6	–	−4.9	−4.9
	C1	2.05	−29.6	−13.5	−31.7	–	−4.9	29.6
	A1	0.49	−6.1	26.3	16.4	–	−6.7	−24.0
T300/3501	Q2	1.00	−11.6	8.8	−17.6	–	−8.1	−8.1
	C2	1.97	−24.1	11.1	−28.1	–	−7.4	25.3
	A2	0.51	−13.3	12.5	−17.0	–	−14.1	−28.9
T300/1034	Q3	1.00	−6.2	−5.6	−15.0	−7.8	7.4	7.4
T300/914C	Q4	1.00	−14.5	9.3	−11.4	−7.0	−10.8	−10.8
Scotchply 1002	C3	1.37	−27.5	−11.8	−28.3	–	−8.5	−6.0
T300/5208[c]	C4	2.07	−23.9	−17.9	−21.7	–	−8.3	18.0

[a]Error percentage between prediction and measured strengths is defined as 100×(predicted strength − measured strength)/measured strength.
[b]In the collected literatures, the prediction by the DZM were only available for laminates Q3 and Q4 in the collected literature.
[c]For laminate C4, maximum % errors were calculated excluding the questionable experimental data as pointed out by the original authors [2].

Also included in Table 4 are error percentages when anisotropy has not been taken into account (i.e., using Soutis et al. CZM approach). Figure 8(a) and (b) show this in more detailed. Figure 8(a) shows that for the cross-ply laminate C1, CZM overestimates heavily and the error increases as hole diameter to width ratio (D/W) decreases. For the angle-ply A1, Figure 8(b) shows CZM underestimates with bigger discrepancy at smaller D/W. If we define an anisotropy factor H as the ratio E to E', then H is unity for quasi-isotropic lay-up. For C1 and A1, H are 2.05 and 0.49, respectively. It is clear from Table 4 that the error incurred by CZM is smaller if H is closer to unity. As compared with the predictions

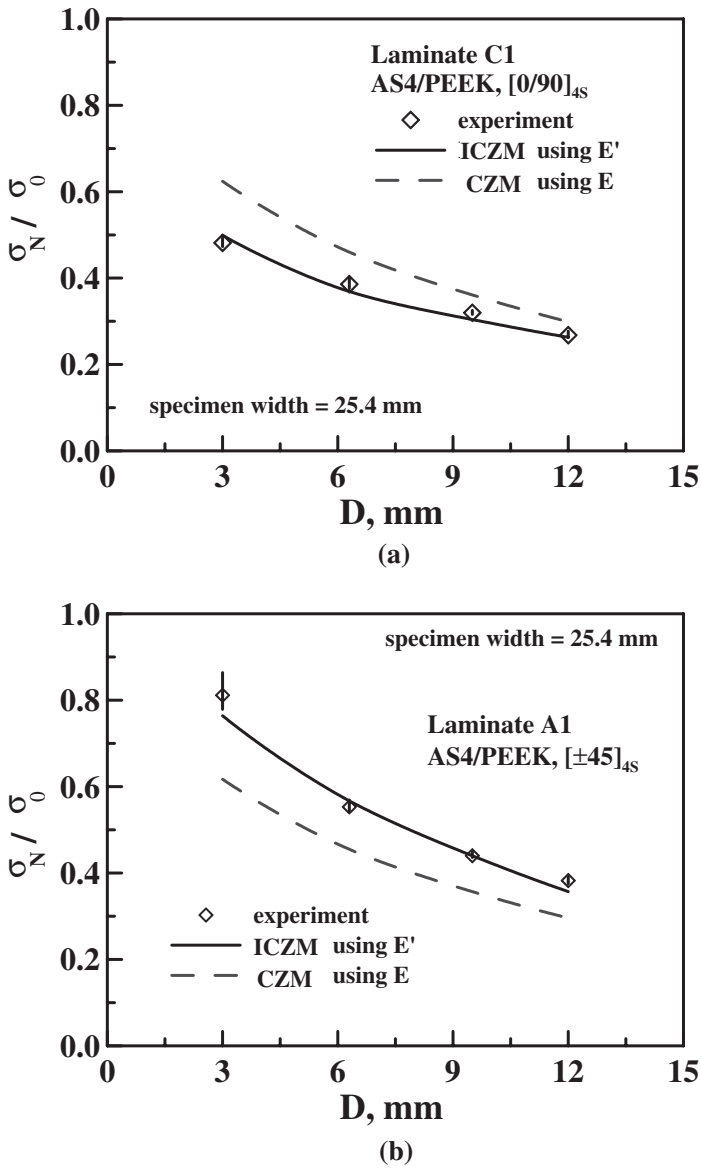

Figure 8. *Residual strength predictions using the longitudinal stiffness E and the effective longitudinal stiffness E′: (a) laminate C1 and (b) laminate A1.*

given by ICZM, CZM will overestimate if $H > 1$ and underestimate if $H < 1$. Incidentally, H for the T800/924C $[\pm 45/0_2]_{3S}$ used by Soutis et al. [19] is 1.2. This may explain why they obtained a favorable prediction even though anisotropy has been ignored. Studies are underway to test this hypothesis further using arbitrary lay-ups-notched laminates under compression.

Progressive Damage Zone

Figure 9 shows the correlation between the normalized applied loading (σ_{app}/σ_0) and the extension of the fictitious crack for our own laminates (Q1, Q2, C1, C2, A1, and A2) with various hole sizes. The lines represent the simulated relationship between σ_{app}/σ_0 and damage zone for various hole sizes. For each laminate, one hole size was chosen to examine the actual damage zone by X-ray or optical microscopic (OM) observation. This observed damage zone size is represented by the diamond symbol in Figure 9. Details of the examination method will be discussed in the next section. After damage initiation at the notch tip, damage zone propagated as the applied stress was increased. When the applied stress reached the maximum value, the corresponding fictitious crack length is defined as the critical damage zone (see solid circle symbols in Figure 9). Apparently, the critical damage zone is not a constant. It increases with the length of the remaining ligament. In other words, the critical damage zone is not a material constant, but is strongly dependent on the specimen configuration, as well as the material properties. This phenomenon is in marked contrast with the basic assumption of the semi-empirical models, which regard the critical damage zone as a material constant. The following damage observation will shed more light on this controversy.

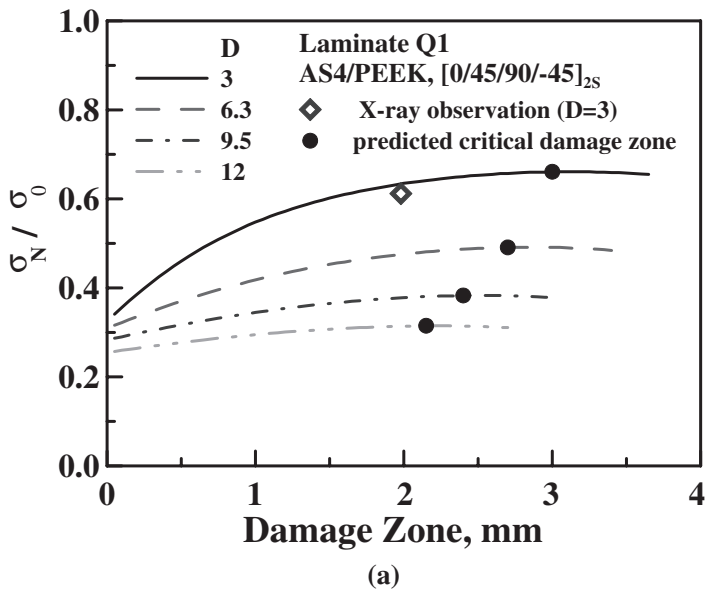

Figure 9. *The correlation between the normalized residual strength and the extension of the fictitious crack for laminates (a) Q1, (b) Q2, (c) C1, (d) C2, (e) A1, and (f) A2 with various hole sizes.*

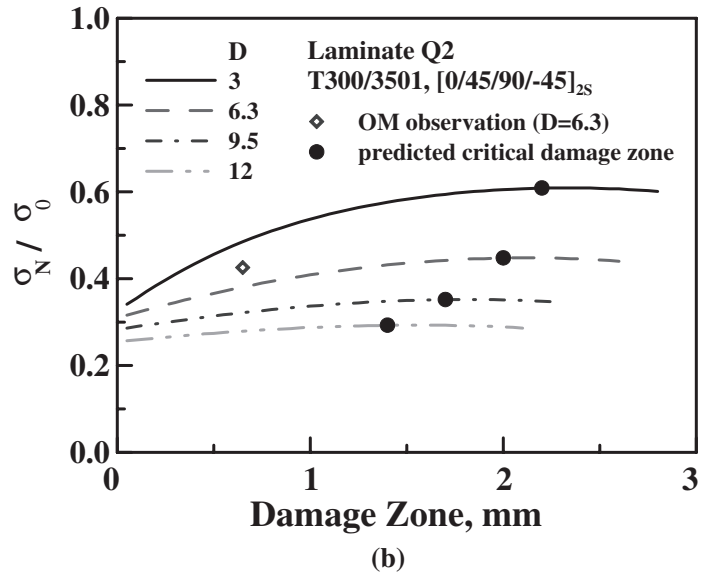

(b)

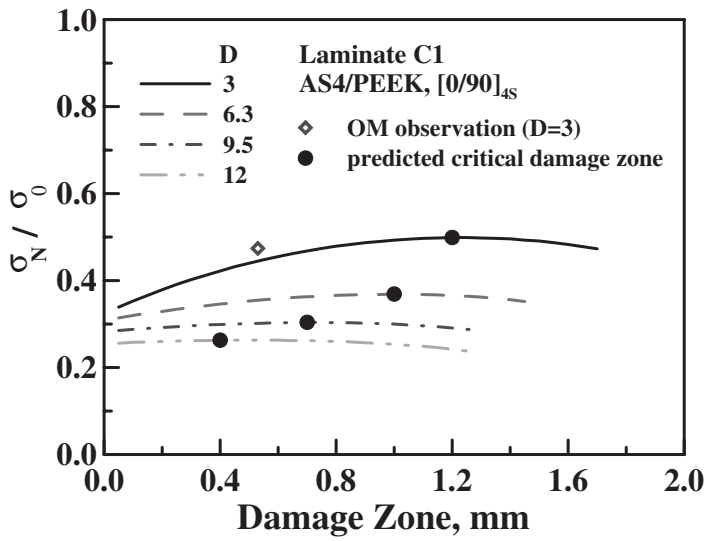

(c)

Figure 9. *Continued.*

Damage Observations

In order to observe the nature and extent of the progressive damage, some specimens were monotonically loaded to specific loads. Tests were then interrupted and the specimens were soaked in zinc iodide (ZnI_2) to prepare for nondestructive examination using X-ray. Figure 10 shows the result of laminate Q1 with a 3 mm-diameter hole, which was loaded to 95% of its failure strength. The damage consists of matrix cracking in the

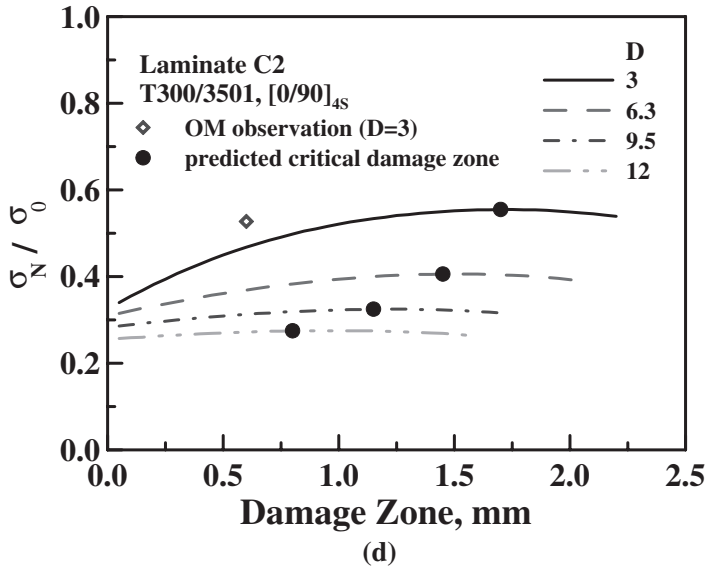

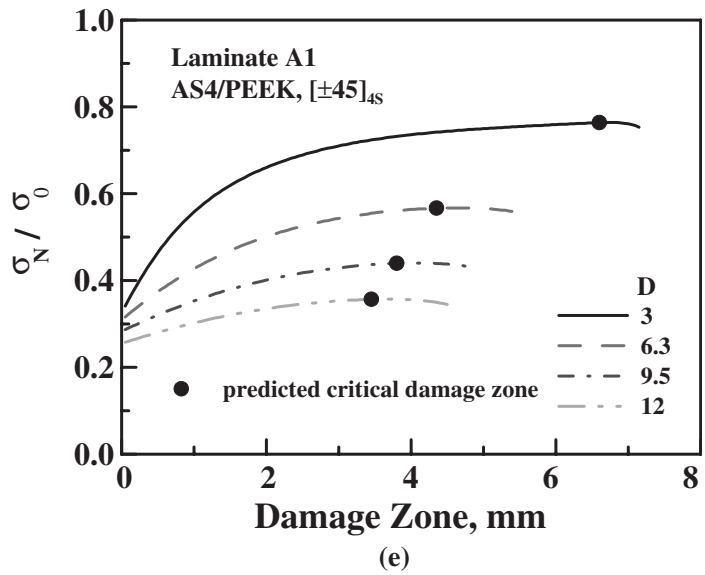

Figure 9. *Continued.*

0°, ±45°, and 90° plies, and delamination among these plies. Delaminations appear as dark shade and matrix crackings as a series of line in the radiograph. If the damage zone is defined as the maximum length projected onto the net-section, the damage zone is around 2 mm under 95% of its failure strength. This information, represented as the diamond symbol in Figure 9(a), corroborated with the predictions by the ICZM. For the cross-ply laminates, no damage was revealed in X-ray radiography even up to 95% of its failure strength. This may be attributed to the fact that the damage was still too small at this load level and the dye had difficultly in penetrating the specimen. Because of the variation in

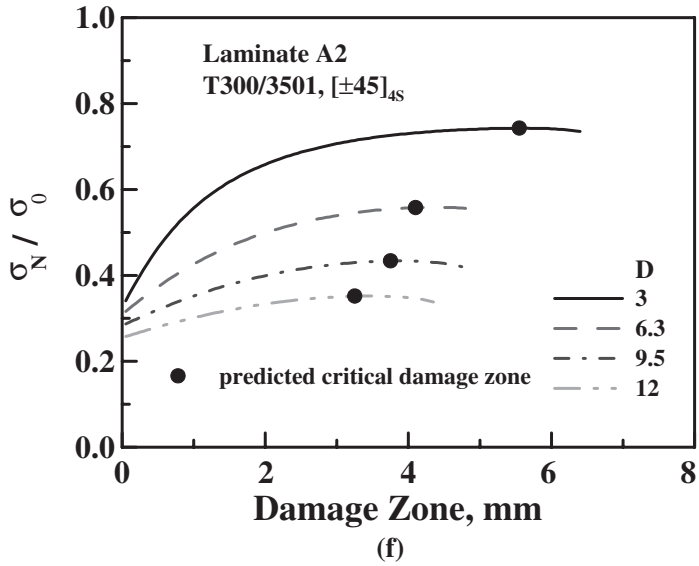

Figure 9. *Continued.*

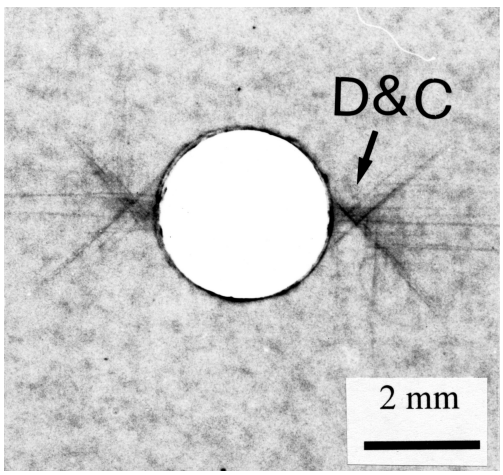

Figure 10. *Matrix cracking and delamination emanating from the notch tip of laminate Q1 at 95% of its failure strength (X-ray observation).*

failure strength from specimen to specimen and that discernible damage only appears very close to catastrophic failure, the success rate of producing samples shown in Figure 10 was extremely low.

A destructive sectioning method, which provides a better resolution for damage observation, was also adopted. Some monotonically loaded specimens were cut at the hole section and were examined using an OM. Mounting of the specimens was so made to expose the edge view of both halves as shown in the inset of Figure 11. Progressively polishing down the mounted sample revealed the extent of damage at different layers and different depths ahead of the notch. Before optical microscope observation, all samples

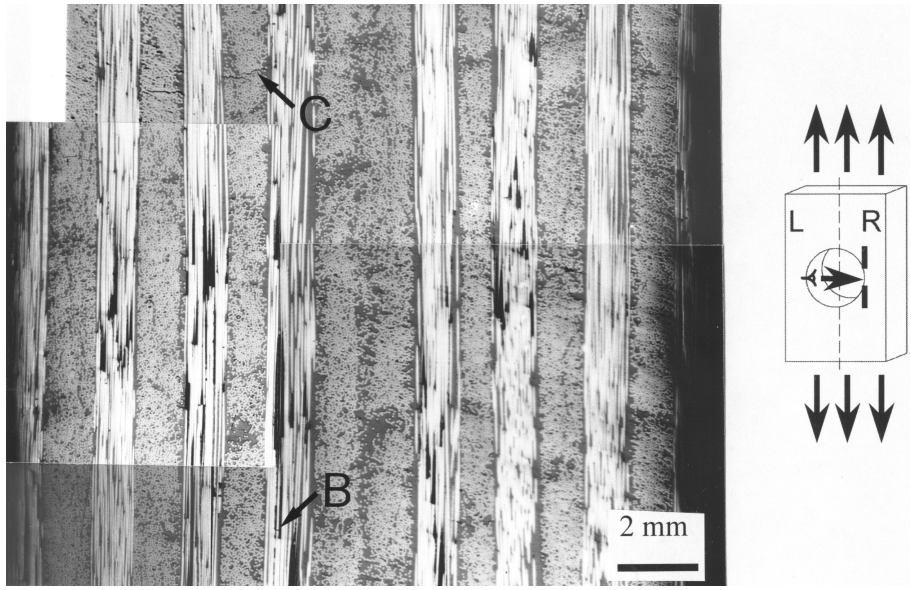

Figure 11. *Matrix cracking and fiber breakage of laminate C1 at 95% of its failure strength (optical microscopy observation).*

were immersed in alcohol, and ultrasonically vibrated to clean off any residual particle inside the damage zone. From the top view of laminate C1 with 3 mm diameter hole, no obvious damage was found. However, the edge view showed obvious fiber breakages (F) in the 0° plies and matrix crackings (C) in the 90° plies were found, as shown in Figure 11. Progressive polishing and examination of this sample revealed that damage no longer exists at 0.55 mm ahead of notch edge. A number of loaded specimens with different stacking sequences were examined this way. The extents of damage zones so revealed were plotted on the relevant figures (see Figure 9(b)–(d)). They are consistent with their counterparts predicted by the ICZM. The above results confirm that the material constant assumption of critical damage zone in many of the existing semi-empirical models should be seriously re-considered.

Good correlation between the observed damage zone size and the ICZM predictions is obtained in all quasi-isotropic and cross-ply lay-ups. However, for the angle-ply laminates (A1 and A2) the damage zones were observable with the naked eyes and were invariably propagating through the net-section of the specimen before failure loads were reached. This may be attributed to the inherently nonlinear deformation behavior of the $[\pm 45]_{4S}$ lay-up. Nevertheless, the ICZM still gives accurate predictions of residual strengths.

CONCLUSIONS

A fictitious crack growth model taking into account of anisotropy has been developed to assess the residual strength of notched composite laminates. The parameters needed: G_c, E', and σ_0, can respectively be measured unambiguously from coupon specimens with and without central slit. Residual strengths of notched AS4/PEEK and T300/3501 composite

laminates with $[0/45/90/-45]_{2S}$, $[0/90]_{4S}$, and $[\pm 45]_{4S}$ lay-ups, and a number of notched laminates from the literatures have been evaluated with good accuracy. If anisotropy has not been accounted for, accuracy in residual strength prediction in cross-ply and angle-ply will be seriously degraded.

For this new model, the damage zones size at different applied loading can be evaluated. The critical damage zone is found to be strongly dependent on the specimen configuration and is not a material constant. The observed damage zones in the laminates with quasi-isotropic and cross-ply lay-ups agree well with the predictions.

ACKNOWLEDGMENTS

The authors appreciate the financial support provided by the National Science Council through the projects NSC88-2212-E-002-041 and NSC89-2218-E002-035.

APPENDIX

Anisotropic Linear Elastic Fracture Mechanics

Consider a plane cracked anisotropic material with a through-thickness crack along the x-axis. The stress–strain relations for the generalized plane stress case are:

$$\begin{Bmatrix} \varepsilon_x \\ \varepsilon_y \\ \gamma_{xy} \end{Bmatrix} = \begin{bmatrix} a_{11} & a_{12} & a_{16} \\ a_{12} & a_{22} & a_{26} \\ a_{16} & a_{26} & a_{66} \end{bmatrix} \begin{Bmatrix} \sigma_x \\ \sigma_y \\ \sigma_{xy} \end{Bmatrix} \tag{A1}$$

where a_{ij} are compliance coefficients. The general solutions for the stresses and displacements near the crack tip are [30]:

$$\sigma_x = \frac{K_I}{\sqrt{2\pi r}} \mathrm{Re}\left[\frac{s_1 s_2}{s_1 - s_2}\left(\frac{s_2}{(\cos\theta + s_2 \sin\theta)^{1/2}} - \frac{s_1}{(\cos\theta + s_1 \sin\theta)^{1/2}}\right)\right] \tag{A2a}$$

$$\sigma_y = \frac{K_I}{\sqrt{2\pi r}} \mathrm{Re}\left[\frac{1}{s_1 - s_2}\left(\frac{s_1}{(\cos\theta + s_2 \sin\theta)^{1/2}} - \frac{s_2}{(\cos\theta + s_1 \sin\theta)^{1/2}}\right)\right] \tag{A2b}$$

$$\sigma_{xy} = \frac{K_I}{\sqrt{2\pi r}} \mathrm{Re}\left[\frac{s_1 s_2}{s_1 - s_2}\left(\frac{1}{(\cos\theta + s_1 \sin\theta)^{1/2}} - \frac{1}{(\cos\theta + s_2 \sin\theta)^{1/2}}\right)\right] \tag{A2c}$$

and

$$v_x = K_I \sqrt{2\pi r} \mathrm{Re}\left\{\frac{1}{s_1 - s_2}\left[s_1 p_2 (\cos\theta + s_2 \sin\theta)^{1/2} - s_2 p_1 (\cos\theta + s_1 \sin\theta)^{1/2}\right]\right\} \tag{A3a}$$

$$v_y = K_I \sqrt{2\pi r} \mathrm{Re}\left\{\frac{1}{s_1 - s_2}\left[s_1 q_2 (\cos\theta + s_2 \sin\theta)^{1/2} - s_2 q_1 (\cos\theta + s_1 \sin\theta)^{1/2}\right]\right\} \tag{A3b}$$

where $K_I = \sigma\sqrt{\pi d}$ is the mode I stress intensity factor (SIF) and is independent on the material property, and s_i $(i = 1, \ldots, 4)$ are the roots of the characteristic equation

$$a_{11}s^4 - 2a_{16}s^3 + (2a_{12} + a_{66})s^2 - 2a_{26}s + a_{22} = 0 \tag{A4}$$

and

$$p_1 = a_{11}s_1^2 - a_{16}s_1 + a_{12} \qquad p_2 = a_{11}s_2^2 - a_{12}s_2 + a_{12} \tag{A5a}$$

$$q_1 = \frac{a_{12}s_1^2 - a_{26}s_1 + a_{22}}{s_1} \qquad q_2 = \frac{a_{12}s_2^2 - a_{26}s_2 + a_{22}}{s_2} \tag{A5b}$$

In the special case of orthotropic body, the compliance coefficients of a_{16} and a_{26} are equal to zero. The crack opening displacement can be calculated by substituting $\theta = \pi$ into Equation (A3b), and then

$$v_y\big|_{\theta=\pi} = K_I\sqrt{2\pi r}\,\mathrm{Re}\left[\frac{i}{s_1 - s_2}(s_1q_2 - s_2q_1)\right] \tag{A6}$$

For orthotropic body, Equation (A6) become

$$v_y\big|_{\theta=\pi} = 2K_I\sqrt{2\pi r}\left\{\left(\frac{a_{11}a_{22}}{2}\right)^{1/2}\left[\left(\frac{a_{22}}{a_{11}}\right)^{1/2} + \left(\frac{2a_{12} + a_{66}}{2a_{11}}\right)\right]^{1/2}\right\} \tag{A7}$$

Equation (A7) can also be expressed using engineering constants, as

$$v_y\big|_{\theta=\pi} = 2K_I\sqrt{2\pi r}\left\{\frac{1}{\sqrt{2E_{xx}E_{yy}}}\left[\sqrt{\frac{E_{xx}}{E_{yy}}} + \frac{E_{xx}}{2G_{xy}} - \nu_{xy}\right]^{1/2}\right\} \tag{A8}$$

To make a comparison of crack opening displacement (COD) between orthotropic and isotropic bodies, the Young's modulus E has to be replaced by the effective longitudinal stiffness E', if the COD of an isotropic body is used to substitute its orthotropic counterpart. E' is expressed as

$$E' = \left\{\frac{1}{\sqrt{2E_{xx}E_{yy}}}\left[\sqrt{\frac{E_{xx}}{E_{yy}}} + \frac{E_{xx}}{2G_{xy}} - \nu_{xy}\right]^{1/2}\right\}^{-1} \tag{A9}$$

REFERENCES

1. Whitney, J.M. and Nuismer, R.J. (1974). Stress Fracture Criteria for Laminated Composites Containing Stress Concentrations, *Journal of Composite Materials*, **8**: 253–265.
2. Nuismer, R.J. and Whitney, J.M. (1975). Uniaxial Failure of Composite Laminates Containing Stress Concentrations, *Fracture Mechanics of Composites*, ASTM STP **593**: 117–142.

3. Karlak, R.F. (1979). Hole Effects in a Related Series of Symmetrical Laminates, In: *Proceeding 4th Joint ASM, Metallurgical Society of the American Institute of Mining Metallurgical and Petroleum Engineers*, Warrendale, PA, pp. 105–117.
4. Byron Pipes, R., Wetherhold, Robert C. and Gillespie, Jr., John W. (1979). Notched Strength of Composite Materials, *Journal of Composite Materials*, **13**: 148–160.
5. Tan, S.C. (1987). Notched Strength Prediction and Design of Laminated Composites Under In-plane Loading, *Journal of Composite Materials*, **21**: 750–780.
6. Tan, S.C. (1987). Laminated Composites Containing an Elliptical Opening. I. Approximate Stress Analysis and Fracture Modes, *Journal of Composite Materials*, **21**: 925–948.
7. Mar, J.W. and Lin, K.Y. (1977). Fracture Mechanics Correlation for Tensile Fracture of Filamentary Composite with Hole, *Journal of Aircraft*, **14**: 703–704.
8. Awerbuch, Jonathan and Madhukar, Madhu S. (1985). Notched Strength of Composite Laminates: Predictions and Experiments – A Revies, *Journal of Reinforced Plastics and Composites*, **4**: 3–159.
9. Bäcklund, Jan (1981). Fracture Analysis of Notched Composites, *Computers and Structures*, **13**: 145–154.
10. Bäcklund, Jan and Aronsson, Carl-Gustaf (1986). Tensile Fracture of Laminates with Hole, *Journal of Composite Materials*, **20**: 259–286.
11. Eriksson, Invar and Aronsson, Carl-Gustaf (1990). Strength of Tensile Loaded Graphite/Epoxy Laminates Containing Cracks, Open and Filled Holes, *Journal of Composite Materials*, **24**: 456–482.
12. Dugdale, D.S. (1960). Yielding of Steel Sheets Containing Slits, *Journal of Mechanics and Physics of Solids*, 100–104.
13. Afaghi-Khatibi, Akbar, Ye, Lin and Mai, Yiu-Wing (1996). An Effective Crack Growth Model for Residual Strength Evaluation of Composite Laminates with Circular Holes, *Journal of Composite Materials*, **30**(2): 142–163.
14. Afaghi-Khatibi, Akbar, Ye, Lin and Mai, Yiu-Wing (1996). Effective Crack Growth and Residual Strength of Composite Laminates with a Sharp Notch, *Journal of Composite Materials*, **30**(3): 333–357.
15. Afaghi-Khatibi, Akbar and Ye, Lin (1996). Notched Strength and Effective Crack Growth in Woven Fabric Composite Laminates with Circular Hole, *Journal of Reinforced Plastics and Composites*, **15**: 344–359.
16. Chang, F.K. and Chang, K.Y. (1987). A Progressive Damage Model for Laminated Composites Containing Stress Concentrations, *Journal of Composite Materials*, **21**: 834–855.
17. Chang, F.K. and Lessard, L.B. (1991). Damage Tolerance of Laminated Composites Containing an Open Hole and Subjected to Compossive Loadings: Part I: Analysis, *Journal of Composite Materials*, **25**: 2–43.
18. Chang, K.Y., Liu, S. and Chang, F.K. (1991). Damage Tolerance of Laminated Composites Containing an Open Hole and Subjected to Tensile Loadings, *Journal of Composite Materials*, **25**: 274–301.
19. Soutis, C., Fleck, N.A. and Smith, P.A. (1991). Failure Prediction Technique for Compression-Loaded Carbon Fiber-Epoxy Laminate with Open Holes, *Journal of Composite Materials*, **25**(11): 1476–1498.
20. Dugdale, D.S. (1960). Yielding of Steel Sheets Containing Slits, *Journal of the Mechanics and Physics of Solids*, **8**: 100–104.
21. Hillerborg, A., Modèer, M. and Petersson, P.-E. (1976). Analysis of Crack Formation and Crack Growth in Concrete by Means of Fracture Mechanics and Finite Elements, *Cement and Concrete Research*, **6**: 773–782.
22. Konish, H.J., Jr. (1975). Mode I Stress Intensity Factors for Symmetrically-Cracked Orthotropic Strips, In: *Fracture Mechanics of Composites*, ASTM STP 593, pp. 99–116.
23. Wang, C.M. (October 2001). Damage Behaviors of Notched Composite Laminates, PhD Dissertation, Department of Mechanical Engineering, National Taiwan University, Taipei, Taiwan.

24. Wang, C.M. and Shin, C.S. Residual Strength Predictions of Composite Laminates with Sharp Slits Using An Improved Cohesive Zone Model, submitted to Journal of Composite Materials.
25. Tan, S.C. (1987). Notched Strength Prediction and Design of Laminated Composites under In-Plane Loadings, *Journal of Composite Materials*, **21**: 750–780.
26. Naik, N.K. and Shembekar, P.S. (1992). Notched Strength of Fabric Laminates, I: Prediction, *Composites Science and Technology*, **44**: 1–12.
27. Belmonte, H.M.S., Manger, C.I.C., Ogin, S.L., Smith, P.A. and Lewin, R. (2001). Characterisation and Modelling of the Notched Tensile Fracture of Woven Quasi-isotropic GFRP Laminates, *Composites Science and Technology*, **61**: 585–597.
28. Coats, T.W. and Harris, C.E. (1998). A Progressive Damage Methodology for Residual Strength Predictions of Notched Composite Panels, NASA/TM-1998- 207646, National Aeronautics and Space Administration, Langley Research Center, Hampton, Virginia 23681–2199.
29. ASTM D3039. Standard Test Method for Tensile Properties of Polymer Matrix Composite Materials, *Annual Book of ASTM Standards*, pp. 111–121.
30. Sih, G.C. and Liebiwutz, H. (1968). Mathematical Theories of Brittle Fracture, Fracture—An Advanced Treatise, Volume II: Mathematical Fundamental, Chapter 2, H. Liebiwutz Ed., Academic Press.